Materials Today Bio 23 (2023) 100805

Contents lists available at ScienceDirect

Materials Today Bio

journal homepage: www.journals.elsevier.com/materials-today-bio

The matrix microenvironment influences but does not dominate tissue-specific stem cell lineage differentiation

Yixuan Amy Pei [a,b], Elmira Mikaeiliagah [a,c], Bin Wang [a,d], Xiaobing Zhang [e,*], Ming Pei [a,f,**]

[a] Stem Cell and Tissue Engineering Laboratory, Department of Orthopaedics, West Virginia University, Morgantown, WV, USA
[b] Perelman School of Medicine, University of Pennsylvania, Philadelphia, PA, USA
[c] Department of Biology, Ardabil Branch, Islamic Azad University, Ardabil, Iran
[d] Department of Foot and Hand Surgery, Clinical Medical College of Yangzhou University, Subei People's Hospital of Jiangsu Province, Yangzhou, Jiangsu, China
[e] Haihe Laboratory of Cell Ecosystem, Institute of Hematology & Blood Diseases Hospital, Peking Union Medical College, Tianjin, China
[f] WVU Cancer Institute, Robert C. Byrd Health Sciences Center, West Virginia University, Morgantown, WV, USA

ARTICLE INFO

Keywords:
Decellularized extracellular matrix
Synovium-derived MSCs
Adipose-derived MSCs
Chondrogenesis
Adipogenesis

ABSTRACT

Mesenchymal stem cells (MSCs) play a pivotal role in tissue engineering and regenerative medicine, with their clinical application often hindered by cell senescence during *ex vivo* expansion. Recent studies suggest that MSC-deposited decellularized extracellular matrix (dECM) offers a conducive microenvironment that fosters cell proliferation and accentuates stem cell differentiation. However, the ability of this matrix environment to govern lineage differentiation of tissue-specific stem cells remains ambiguous. This research employs human adipose-derived MSCs (ADSCs) and synovium-derived MSCs (SDSCs) as models for adipogenesis and chondrogenesis differentiation pathways, respectively. Genetically modified dECM (GMdECM), produced by SV40LT-transduced immortalized cells, was studied for its influence on cell differentiation. Both types of immortalized cells displayed a reduction in chondrogenic ability but an enhancement in adipogenic potential. ADSCs grown on ADSC-deposited dECM showed stable chondrogenic potential but increased adipogenic capacity; conversely, SDSCs expanded on SDSC-generated dECM displayed elevated chondrogenic capacity and diminished adipogenic potential. This cell-dependent response was confirmed through GMdECM expansion, with SDSCs showing enhanced chondrogenesis. However, ADSCs did not exhibit improved chondrogenic potential on GMdECM, suggesting that the matrix microenvironment does not dictate the final differentiation path of tissue-specific stem cells. Potential molecular mechanisms, such as elevated basement membrane protein expression in GMdECMs and dynamic TWIST1 expression during expansion and chondrogenic induction, may underpin the strong chondrogenic differentiation of GMdECM-expanded SDSCs.

1. Introduction

Mesenchymal stem cells (MSCs) possess considerable potential for application in tissue regeneration therapies [1]. As these regenerative endeavors often require substantial quantities of MSCs, *ex vivo* expansion is a crucial step. However, this process often culminates in MSC senescence, a state in which cells lose their proliferative and differentiation capabilities [2]. Therefore, overcoming this obstacle is pivotal for successful clinical translation. Emerging evidence suggests that the decellularized extracellular matrix (dECM) generated by MSCs may provide an environment that effectively enhances stem cell proliferation and differentiation capacities [3–5]. However, the extent to which dECM can dictate the lineage differentiation of expanded MSCs remains to be fully understood.

Recent research indicated that human infrapatellar fat pad-derived MSCs (IPFSCs), upon transduction with simian virus 40 large T antigen (SV40LT), displayed enhanced adipogenic differentiation but reduced chondrogenic differentiation [6]. Interestingly, high-passage (senescent) IPFSCs grown on dECM from SV40LT-transduced IPFSCs (termed genetically modified dECM or GMdECM) [7] demonstrated significantly heightened chondrogenic differentiation and diminished adipogenic differentiation compared to their counterparts grown on

* Co-corresponding author. Peking Union Medical College, Tianjin, China.
** Corresponding author. Stem Cell and Tissue Engineering Laboratory, Department of Orthopaedics, West Virginia University, PO Box 9196, 64 Medical Center Drive, Morgantown, WV, 26506, USA.
E-mail addresses: zhangxbhk@gmail.com (X. Zhang), mpei@hsc.wvu.edu (M. Pei).

https://doi.org/10.1016/j.mtbio.2023.100805
Received 7 July 2023; Received in revised form 25 August 2023; Accepted 15 September 2023
Available online 16 September 2023

dECM or tissue culture plastic (TCP) [6]. Nevertheless, it remains unclear whether the observed enhancement in chondrogenic differentiation is inherent to the expanded IPFSCs or driven by the dECM/GMdECM substrate. Considering that IPFSCs demonstrate a predisposition for chondrogenic differentiation over adipose-derived MSCs (ADSCs) from the subcutaneous fat pad [8] and their dual differentiation potential, they may not serve as an ideal MSC model for examining the influence of the matrix microenvironment on tissue-specific stem cell lineage differentiation.

In this study, we utilized two tissue-specific stem cells, ADSCs, which are known for robust adipogenic but weak chondrogenic potential, and synovium-derived MSCs (SDSCs), which are noted for their pronounced chondrogenic but limited adipogenic differentiation [8–10]. Our aim was to investigate whether the matrix microenvironment, be it dECM or GMdECM, steers the lineage differentiation of expanded MSCs. Our findings echoed previous reports on SV40LT-transduced IPFSCs [6,11], showing that both ADSCs and SDSCs, when transduced with SV40LT, exhibited diminished chondrogenic potential but amplified adipogenic capacity. Furthermore, we observed that dECM generated by SV40LT-transduced SDSCs greatly enhanced the chondrogenic capacity of SDSCs but reduced their adipogenic potential. Conversely, dECM deposited by SV40LT-transduced ADSCs markedly bolstered ADSC adipogenic capacity, with no substantial change in chondrogenic potential. Interestingly, SDSCs cultured on GMdECMs derived from SV40LT-transduced ADSCs/SDSCs exhibited more pronounced enhancement in chondrogenic differentiation compared to a modest increase observed in expanded ADSCs. Our results collectively suggest that while the matrix microenvironment influences the lineage differentiation of tissue-specific stem cells, it does not solely dictate this process.

2. Materials and methods

2.1. Study design

This research was designed in three sections:

(i) In the TCP culture regimen, we used human adult ADSCs and SDSCs transduced with SV40LT or green fluorescent protein (GFP) lentivirus vectors as detailed in previous protocols, labeled SV40LT and G-CTR, respectively. We designated non-transduced cells as controls (CTR). The series of investigations involved the use of immunofluorescence staining to confirm successful transduction, flow cytometry to characterize surface markers post-SV40LT transduction, reverse transcription quantitative PCR (RT–qPCR) to assess stemness- and senescence-related gene expression, and Alcian blue (Ab) staining, immunohistochemistry (IHC) staining, Western blotting, and RT–qPCR to evaluate chondrogenic and adipogenic differentiation.

(ii) For the first dECM culture regimen, to determine whether dECM influenced stem cell lineage differentiation, we cultured Passage 5 (P5) ADSCs and P6 SDSCs on the dECM deposited by their corresponding MSCs transduced with SV40LT (sECM) or GFP (gECM) or non-transduced controls (cECM), with TCP serving as a non-dECM control. Following cell expansion on these substrates, we planned experiments that included immunofluorescence staining for evaluating the expression of basement membrane proteins in gECM/sECM, RT–qPCR for determining the expression of epithelial-mesenchymal transition (EMT) transcription factors, and Ab staining, IHC staining, Western blotting, and RT–qPCR for assessing chondrogenic and adipogenic differentiation.

(iii) For the second dECM culture regimen, to determine whether dECM dominated stem cell lineage differentiation, we expanded P5 SDSCs and P6 ADSCs on dECM deposited by SV40LT-transduced SDSCs and ADSCs (SE40 and AE40, respectively), using TCP as a control. We employed Ab and IHC staining and RT–qPCR to assess chondrogenic differentiation of ADSCs and SDSCs after expansion on GMdECMs.

2.2. SV40LT transduction

This study received the necessary approval from the Institutional Biosafety Committee. Human adult SDSCs from two male and two female donors (average age of 43 years old) and ADSCs from multiple female donors (average age of 43 years old) (cat no. ASC-F-SL, ZenBio Inc, Research Triangle Park, NC) [12,13] underwent transduction with either SV40LT (pRSC-EF1-SV40LT-E2A-Puro-wpre) or GFP (pRSC-EF1-Puro-E2A-GFP-wpre) lentiviral vectors. The transduction was carried out in complete medium composed of alpha minimum essential medium (αMEM) supplemented with 10% fetal bovine serum (FBS), 100 U/mL penicillin, 100 μg/mL streptomycin, and 0.25 μg/mL fungizone (Invitrogen, Carlsbad, CA). After incubating for 24 h, selection was performed with 2 μg/mL puromycin over a 4-day period.

The success of SV40LT lentivirus transduction in human adult ADSCs and SDSCs was verified by immunocytochemistry staining. Briefly, 0.3×10^5 cells that had been seeded on a gelatin precoated tissue culture coverslip (Neuvitro Corporation, Vancouver, WA) were fixed with 4% paraformaldehyde for 15 min. This step was followed by permeabilization using 1% Triton X-100 in phosphate-buffered saline (PBS). After blocking with a reagent consisting of 10% normal horse serum and 0.1% Triton X-100 in PBS, cells were exposed to SV40 T Ag primary antibody (Table 1), followed by an Alexa Fluor Plus 555-conjugated anti-mouse secondary antibody (cat no. A-32773, Invitrogen). We evaluated the fluorescence intensity of each group using a Zeiss Axiovert 40 CFL Inverted Microscope (Zeiss Oberkochen, Germany).

2.3. dECM preparation and matrix staining

The preparation of the dECM followed a previously established protocol [14]. In brief, TCP was initially precoated with 0.2% gelatin (MilliporeSigma, Burlington, MA) at 37 °C for 1 h. Subsequent treatments included 1% glutaraldehyde (MilliporeSigma) and 1 M ethanolamine (MilliporeSigma), each for 30 min. Passage 8 ADSCs and Passage 9 SDSCs, transduced with SV40LT or GFP lentivirus, or non-transduced, were cultured on the precoated TCP until reaching full confluence. At this stage, 250 μM L-ascorbic acid phosphate (Wako Chemicals USA, Richmond, VA) was added to the complete medium [15]. Following a 7-day incubation period, the cells were removed by the addition of 0.5% Triton X-100 containing 20 mM ammonium hydroxide (Sargent-Welch, Skokie, IL) at 37 °C for 5 min. The resulting dECM was stored in PBS supplemented with 100 U/mL penicillin, 100 μg/mL streptomycin, and 0.25 μg/mL fungizone at 4 °C until further use.

Table 1
Summary of primary antibodies.

Application	Antibody	Company	Cat. no.
Flow cytometry	CD73-APC	eBioscience	17-0739-42
	CD90-APC-Vio® 770	Miltenyi Biotec	130-114-863
	CD105-PerCp-Vio® 700	eBioscience	130-112-170
	CD146-PE	eBioscience	12-1469-42
Immunohistochemistry	ALPL	DSHB	B4-78
	Collagen I [COL-1]	GeneTex	GTX26308
	Collagen II	DSHB	II6B3-c
	Collagen X	GeneTex	GTX37732
Immunofluorescence	Collagen IV	DSHB	M3F7
	Fibronectin	DSHB	HFN 7.1
	Laminin	Invitrogen	PA1-16730
	Nidogen 1 (C-7)	Santa Cruz	Sc-133,175
	Perlecan (A7L6)	Santa Cruz	Sc-33707
	SV40 T Ag	Santa Cruz	Sc-147

For matrix staining, the dECM was fixed with 4% paraformaldehyde and blocked using 1% bovine serum albumin (BSA). The matrix was then incubated overnight at 4 °C with primary antibodies targeting fibronectin, collagen IV, nidogen 1, perlecan, and laminin (Table 1). After washing with PBS, the dECM was subjected to secondary antibodies: Alexa Fluor Plus 555-conjugated anti-mouse secondary antibody (Invitrogen) for the detection of fibronectin, collagen IV, and nidogen 1, Alexa Fluor 488-conjugated anti-rabbit secondary antibody (cat no. A-11008, Invitrogen) for laminin detection, and Alexa Fluor 488-conjugated anti-rat secondary antibody (cat no. A-11006, Invitrogen) for perlecan detection. The fluorescence intensity of each group was measured using a Zeiss Axiovert 40 CFL Inverted Microscope (Zeiss Oberkochen).

2.4. Assessment of surface markers, cellular proliferation (EdU), and stemness gene expression

Cell surface marker analysis was conducted on 4×10^5 expanded cells from each group, initially immersed in cold PBS enriched with 0.1% ChromPure Human IgG, whole molecule (code no. 009-000-003, Jackson ImmunoResearch Laboratories, West Grove, PA) for 30 min. Thereafter, the cells were incubated with primary antibodies against the MSC surface markers CD73, CD90, CD105, and CD146 (Table 1) in the dark at 4 °C for 30 min. The fluorescence analysis was carried out by a BD FACSCalibur™ flow cytometer (BD Biosciences, San Jose, CA) with data interpretation facilitated by the FCS Express 7 Research Edition (De Novo Software, Los Angeles, CA).

Cellular proliferation capacity was evaluated using the Click-iT™ EdU (5-ethynyl-2′-deoxyuridine) Alexa Fluor™ 647 Flow Cytometry Assay Kit (cat no. C10419, Invitrogen). Upon reaching 45% confluence, cells were treated with EdU at a final concentration of 10 μM and incubated at 37 °C for 20 h. Cells harvested from each group (3×10^5) were washed twice with PBS containing 1% BSA and fixed in 180 μL of 0.4% paraformaldehyde. After a 15-min incubation in a dark room, the cells were treated with 1 × Click-iT™ reaction cocktail and kept in the dark for an additional 30 min. Fluorescence was assessed using a BD FACSCalibur™ flow cytometer (BD Biosciences), and data were analyzed with the FCS Express 7 Research Edition (De Novo Software).

For the examination of stemness gene expression, total RNA from cell samples (n = 3) was extracted using an RNase-free pestle in TRIzol® reagent (MilliporeSigma). Next, 2 μg of total RNA was reverse transcribed using the High-Capacity cDNA Reverse Transcription Kit at 37 °C for 120 min, as per the manufacturer's instructions (Thermo Fisher Scientific, Foster City, CA). A qPCR procedure was employed to assess the expression of stemness-related genes (MYC, KLF4, POU5F1, NES, NOV, NANOG, SOX2, BMI1), senescence-related genes (TP53, CDKN1A, CDKN2A), and EMT transcription factors (TWIST1, ZEB1, SNAIL1) using GAPDH (Glyceraldehyde 3-phosphate dehydrogenase) as the endogenous control gene (Table 2). qPCR was executed using the Applied Biosystems™ 7500 Fast Real-Time PCR System (Thermo Fisher Scientific) under the following conditions: 50 °C for 2 min, hot start at 95 °C for 10 min followed by 40 cycles of denaturation at 95 °C for 15 s and annealing and extension at 60 °C for 1 min. Relative transcript levels were calculated as $\chi = 2^{-\Delta\Delta Ct}$, where $\Delta\Delta Ct = \Delta E - \Delta C$, $\Delta E = Ct_{exp} - Ct_{GAPDH}$, and $\Delta C = Ct_{ct1} - Ct_{GAPDH}$.

2.5. Chondrogenic induction and differentiation evaluation

For chondrogenic induction, expanded cells (0.3×10^6) from each group were subjected to centrifugation at 1200 rpm for 7 min in a 15-mL polypropylene tube to form a pellet. After 24 h of culture in complete medium, the pellets (now referred to as day 0 pellets) were treated with chondrogenic induction medium. This medium was composed of high-glucose Dulbecco's modified Eagle's medium (DMEM), 40 μg/mL proline (MilliporeSigma), 100 μM dexamethasone (MilliporeSigma), 100 U/mL penicillin, 100 μg/mL streptomycin, 0.1 mM L-ascorbic acid-2-phosphate, and 1 × ITS™ Premix (6.25 μg/mL insulin, 6.25 μg/mL transferrin, 6.25 μg/mL selenous acid, 5.35 μg/mL linoleic acid, and 1.25 μg/mL BSA) (BD Biosciences), with the addition of 10 ng/mL transforming growth factor beta 3 (TGF-β3) (PeproTech Inc., Rocky Hill, NJ). The pellets were incubated in this medium at 37 °C and 5% O_2 in a humidified incubator for an additional 10 and 21 days.

The degree of chondrogenic differentiation was evaluated using histology and IHC staining on day 21. Additionally, RT−qPCR was conducted on days 0, 10, and 21 to assess the expression levels of chondrogenic-related genes (SOX9, ACAN, Col2A1, PRG4, COL1A1, COL10A1) and EMT transcription factors (TWIST1, ZEB1, SNAIL1), with GAPDH serving as the endogenous control gene (Table 2). For histology, representative pellets (n = 3) were fixed in a 4% paraformaldehyde solution at 4 °C overnight. Next, the pellets were dehydrated using a gradient ethanol series, cleared with a xylene solution, and embedded in paraffin blocks for slicing. Sections, 5 μm thick, were then stained with Alcian blue (Thermo Fisher Scientific) for sulfated glycosaminoglycan (GAG) detection and counterstained with fast red.

In the IHC staining procedure, consecutive sections were treated with 1% hydrogen peroxide to inhibit endogenous peroxidase activity, incubated with 2 mg/mL hyaluronidase in PBS (pH = 5) at 37 °C for 30 min, and then treated with 1% normal horse serum for 30 min. Subsequently, the sections were probed with primary antibodies against collagens I, II, and X and ALPL (Table 1), followed by application of the secondary antibody, biotinylated horse anti-mouse/rabbit IgG (H + L) (Vector, Burlingame, CA). Immunoactivity was visualized using Vectastain ABC reagent (Vector) with 3,3′-diaminobenzidine (DAB, Vector) as a substrate. Hematoxylin (Vector) was used for counterstaining.

Table 2
Summary of TaqMan PCR marker gene Assay ID.

Marker gene	Gene name	Full name	Assay ID
Stemness	BMI1	B lymphoma Mo-MLV insertion region 1 homolog	Hs00180411_m1
	KLF4	Kruppel-like factor 4	Hs00358836_m1
	MYC	MYC proto-oncogene	Hs00153408_m1
	NANOG	Nanog Homeobox	Hs02387400_g1
	NES	Nestin	Hs04187831_g1
	NOV	Nephroblastoma overexpressed	Hs00159631_m1
	POU5F1	POU class 5 homeobox 1	Hs04260367_gH
	SOX2	(SRY (sex determining region Y)-box 2	Hs01053049_s1
Senescence	CDKN1A	Cyclin dependent kinase inhibitor 1A	Hs00355782_m1
	CDKN2A	Cyclin dependent kinase inhibitor 2A	Hs00923894_m1
	TP53	Tumor protein p53	Hs01034249_m1
Adipogenesis	CEBPA	CCAAT enhancer binding protein alpha	Hs00269972_s1
	FABP4	Fatty acid-binding protein 4	Hs01086177_m1
	LEP	Leptin	Hs00174877_m1
	LPL	Lipoprotein lipase	Hs00173425_m1
	PPARG	Peroxisome proliferator-activated receptor gamma	Hs01115513_m1
	UCP1	Uncoupling protein 1	Hs01084772_m1
Chondrogenesis	ACAN	Aggrecan	Hs00153936_m1
	COL1A1	Collagen I	Hs00164004_m1
	COL2A1	Collagen II	Hs00156568_m1
	COL10A1	Collagen X	Hs00166657_ml
	PRG4	Proteoglycan 4	Hs00981633_m1
	SOX9	SRY-Box 9	Hs00165814_m1
EMT transcription factor	SNAIL1	*Snail* Family Transcriptional Repressor 1	Hs00195591_m1
	TWIST1	Twist Family BHLH Transcription Factor 1	Hs00361186_m1
	ZEB1	Zinc finger E-box-binding homeobox 1	Hs01566410_m1
Housekeeping	GAPDH	Glyceraldehyde-3-phosphate dehydrogenase	Hs02758991_g1

2.6. Adipogenic induction and differentiation evaluation

Adipogenic induction was initiated once the cells achieved 95% confluence. At this stage, the complete medium was replaced with adipogenic induction medium for a 21-day period. This adipogenic medium contained complete medium supplemented with 1 μM dexamethasone (MilliporeSigma), 0.5 mM isobutyl-1-methylxanthine (Fisher Scientific), 200 μM indomethacin (MilliporeSigma), and 10 μM insulin (BioVendor, Asheville, NC). The cells were maintained at 37 °C in a humidified incubator with 5% CO_2.

For staining lipid-filled droplets inside the cells, samples of the induced cells (n = 3) were rinsed with PBS, fixed in 4% formaldehyde for

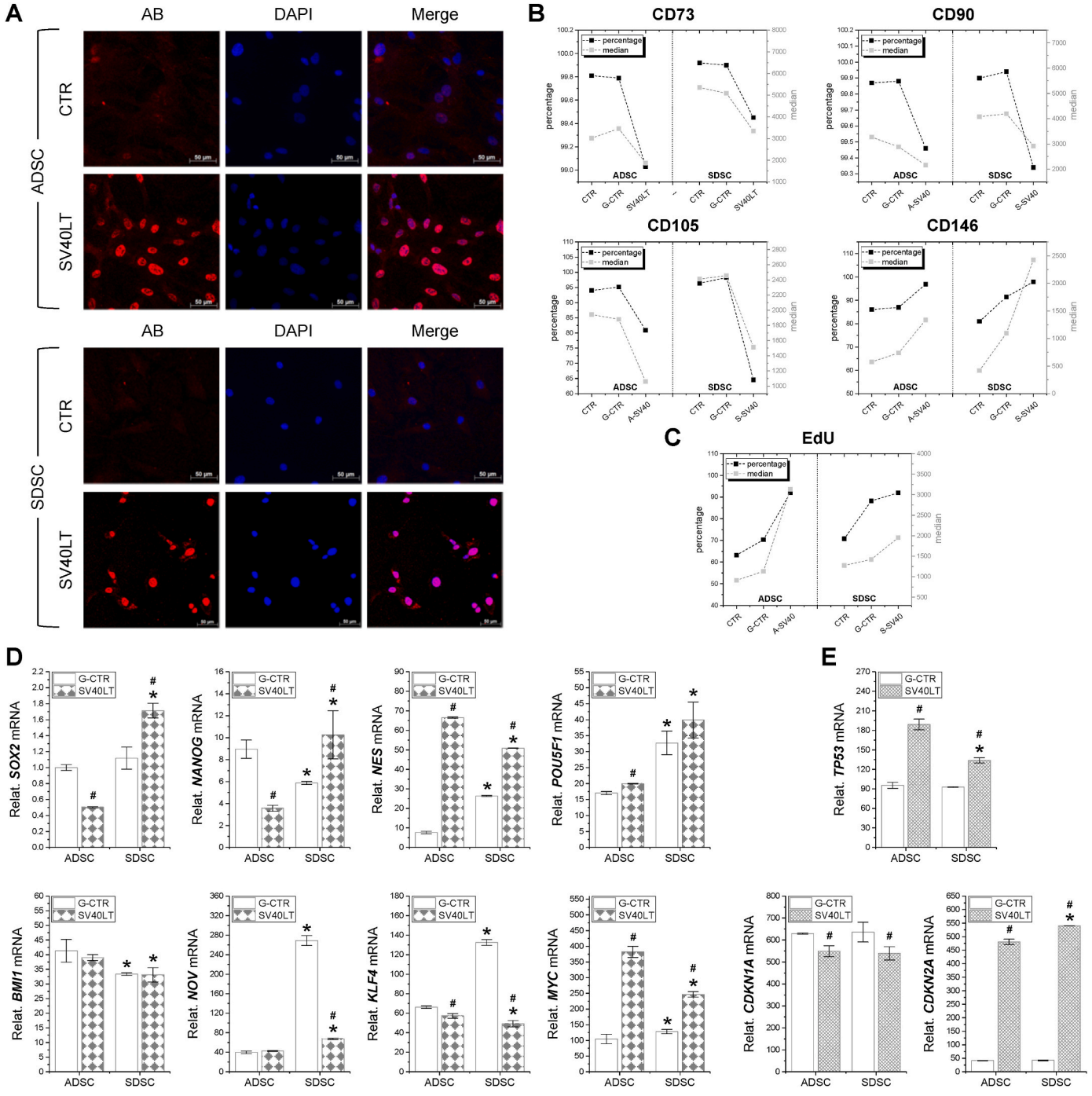

Fig. 1. Influence of SV40LT transduction on the expression of surface markers and stemness/senescence markers in human ADSCs/SDSCs. (A) After transduction and selection with puromycin, intense SV40LT staining (red) was observed in the nuclei of all ADSCs and SDSCs subjected to SV40LT transduction (SV40LT). Nuclei were counterstained with DAPI (blue). Non-transduced cells served as controls (CTR). AB indicates the primary antibody against SV40 T Ag. (B) The expression of surface markers CD73, CD90, CD105, and CD146 was evaluated using flow cytometry in ADSCs/SDSCs transduced with SV40LT (A-SV40/S-SV40), GFP (G-CTR), or without transduction (CTR). (C) Relative EdU incorporation was measured in the same groups. (D) TaqMan® qPCR was used to determine the mRNA expression levels of the stemness markers SOX2, NANOG, NES, POU5F1, BMI1, NOV, KLF4, and MYC in ADSCs/SDSCs subjected to SV40LT (SV40LT) or GFP transduction (G-CTR). (E) The mRNA expression levels of senescence markers TP53, CDKN1A, and CDKN2A were assessed using TaqMan® qPCR. Data are represented as bar charts. The symbol * denotes a statistically significant difference compared to the corresponding ADSC group ($P < 0.05$), while # indicates a significant difference from the corresponding G-CTR group ($P < 0.05$). (For interpretation of the references to colour in this figure legend, the reader is referred to the Web version of this article.)

10 min, and then stained with a fresh 0.6% (w/v) Oil Red O (ORO) (MilliporeSigma) solution (60% Isopropanol, 40% Water) at room temperature for 15 min on a shaker. The cells were then washed with tap water to remove unbound dye and photographed under an Olympus IX51 microscope (Olympus America Inc., Center Valley, PA). RT−qPCR was performed to quantify the mRNA levels of adipogenic marker genes (LPL, FABP4, CEBPA, PPARG, LEP, and UCP1) and EMT transcription factors (TWIST1, ZEB1, and SNAIL1), with GAPDH serving as the endogenous control gene (Table 2).

For semiquantitative analysis at the protein level, induced cell samples (n = 3) were used to extract proteins using lysis buffer (Cell Signaling Technology, Danvers, MA) that included protease inhibitors. Total protein quantification was performed using a Pierce™ BCA Protein Assay Kit (Thermo Fisher Scientific). A total of 30 μg of protein from each sample was loaded onto NuPAGE™ Bis-Tris Mini Gels (Invitrogen) and run on an XCell SureLock Mini-Cell (Thermo Fisher Scientific) at 90 V for 30 min, followed by 120 V for an additional 30 min. Protein bands on the gel were transferred onto a PVDF membrane using an XCell II™ Blot module™ (Thermo Fisher Scientific) at 30 V at 4 °C overnight. Post transfer, the membrane was incubated with primary antibodies targeting FABP4 (Santa Cruz Biotechnology, Dallas, TX) and GAPDH (Thermo Fisher Scientific) in 5% BSA in Tris-buffered saline with 0.1% Tween® 20 detergent (TBST) buffer at 4 °C overnight. The membrane was then incubated with a secondary antibody, horseradish peroxidase-conjugated goat anti-mouse (Invitrogen), for 1 h. Detection was performed using SuperSignal™ West Pico Plus Chemiluminescence Substrate (Thermo Fisher Scientific).

2.7. Statistical analysis

The statistical analysis was carried out using the SPSS 20.0 software package. Pairwise comparisons between groups were performed using the nonparametric Mann−Whitney *U* test. The threshold for statistical significance was set at $P < 0.05$, indicating that differences yielding a P value less than 0.05 were considered statistically significant, demonstrating a high likelihood that the differences observed were not due to chance.

3. Results

3.1. Influence of immortalization on MSC surface markers and stemness/senescence genes

Immunofluorescence staining showed that both ADSCs and SDSCs were intensely positive for SV40LT in the cell nuclei, particularly in cells that had undergone transduction. In contrast, control cells (non-transduced) showed minimal staining for SV40LT (Fig. 1A). To understand the impact of immortalization on the biological properties of MSCs, flow cytometry was used to analyze the expression of MSC surface markers, including CD73, CD90, CD105, and CD146 (Fig. 1B). In addition, the rate of cell proliferation was measured through the incorporation of the thymidine analog EdU (Fig. 1C). We observed that SV40LT-transduced cells showed a decrease in the percentage and median fluorescence intensity (MFI) of CD73, CD90, and CD105. Conversely, SV40LT transduction resulted in increased expression of CD146 and an elevated rate of EdU incorporation.

The impact of SV40LT transduction on the expression of stemness genes was also found to vary with the type of stem cell (Fig. 1D). In both types of stem cells, SV40LT transduction led to increased expression of NES and MYC but a decrease in KLF4. Intriguingly, SOX2 and NANOG showed decreased expression in ADSCs but increased expression in SDSCs after SV40LT transduction. Additionally, SV40LT transduction increased POU5F1 expression exclusively in ADSCs, while only SDSCs showed a reduction in NOV expression. No significant changes were observed in the expression of BMI1 in either transduced cell line. For senescence-related genes (Fig. 1E), SV40LT transduction led to an upregulation of TP53 and CDKN2A and a downregulation of CDKN1A in both types of stem cells.

3.2. Impact of SV40LT immortalization on stem cell lineage differentiation

The effect of immortalization on the chondrogenic differentiation of stem cells was investigated by culturing SV40LT-transduced ADSCs and SDSCs in a pellet culture system with chondrogenic induction medium for 21 days. The resulting cells were assessed via Ab and IHC staining (Fig. 2A/C) and RT−qPCR (Fig. 2B/D). The results indicated that SDSCs demonstrated higher expression of sulfated GAGs and collagen II than ADSCs (CTR in Fig. 2C vs 2A). However, these staining intensities were less pronounced in SV40LT-immortalized SDSCs (SV40LT in Fig. 2C). At the mRNA level, ADSCs exhibited a reduced response to chondrogenic induction compared to SDSCs (Fig. 2B vs 2D), a finding consistent with the histology data (Fig. 2A vs 2C). Furthermore, SV40LT-transduced MSCs from both sources showed a significant decrease in SOX9, ACAN, PRG4, and COL1A1 but not in COL2A1 and COL10A1 (Fig. 2B vs 2D).

The impact of immortalization on the adipogenic differentiation of stem cells was evaluated by culturing SV40LT-transduced ADSCs and SDSCs in adipogenic induction medium for 21 days. Subsequently, the induced cells were assessed via RT−qPCR (Fig. 3A/B), ORO staining (Fig. 3C), and Western blot analysis (Fig. 3D). Adipogenic induction significantly enhanced the expression of PPARG, CEBPA, and FABP4 in SV40LT-transduced ADSCs (Fig. 3A) and LPL, CEBPA, and FABP4 in SV40LT-transduced SDSCs (Fig. 3B). This upregulation was further validated by Western blot analysis of FABP4 expression (Fig. 3C). Additionally, adipogenic induction considerably reduced the white adipose tissue marker LEP while increasing the brown adipose tissue marker UCP1 in SV40LT-transduced SDSCs (Fig. 3D). Compared to the ADSC group, abiogenically induced SDSCs exhibited significantly lower expression of LEP, a trend that remained even in the SV40LT-transduced group (Fig. 3D). Intriguingly, SV40LT-transduced SDSCs showed a significant upregulation of UCP1 mRNA (Fig. 3D). ORO staining revealed that, compared to regular lipid droplets in the corresponding CTR and G-CTR groups, numerous smaller lipid droplets were detected in both SV40LT-transduced ADSC and SDSC groups (Fig. 3E). This change suggests a potential shift toward brown adipose tissue characteristics.

3.3. Basement membrane protein expression in GMdECMs and EMT transcription factor expression during adipogenic and chondrogenic differentiation

The impact of SV40LT transduction on the expression of basement membrane proteins in both ADSCs and SDSCs was investigated using immunofluorescence staining. This analysis identified the expression levels of collagen IV (COL4), laminin (LAM), nidogen 1 (NID1), and perlecan (PLC), along with fibronectin (FN), in sECM and gECM samples (Fig. 4A). No significant difference in FN expression was detected between the gECM and sECM of both stem cell types. Interestingly, the sECM derived from ADSCs displayed slightly higher levels of COL4, NID1, and PLC expression than their gECM counterparts. Even more notably, the sECM derived from SDSCs demonstrated significantly elevated levels of COL4, LAM, NID1, and PLC compared to the corresponding gECM group.

To evaluate the expression of EMT transcription factors in expanded cells and during adipogenic and chondrogenic differentiation, the mRNA levels of TWIST1, ZEB1, and SNAIL1 were quantified using RT−qPCR (Fig. 4B). The results showed that the expression of ZEB1 and SNAIL1 in both ADSCs and SDSCs followed a similar trend during expanded cell proliferation and subsequent differentiation, with the lowest expression observed in chondrogenicly induced SDSCs post sECM expansion. Interestingly, a distinct dynamic was observed in TWIST1 expression in SDSCs. Although ADSCs showed no significant changes

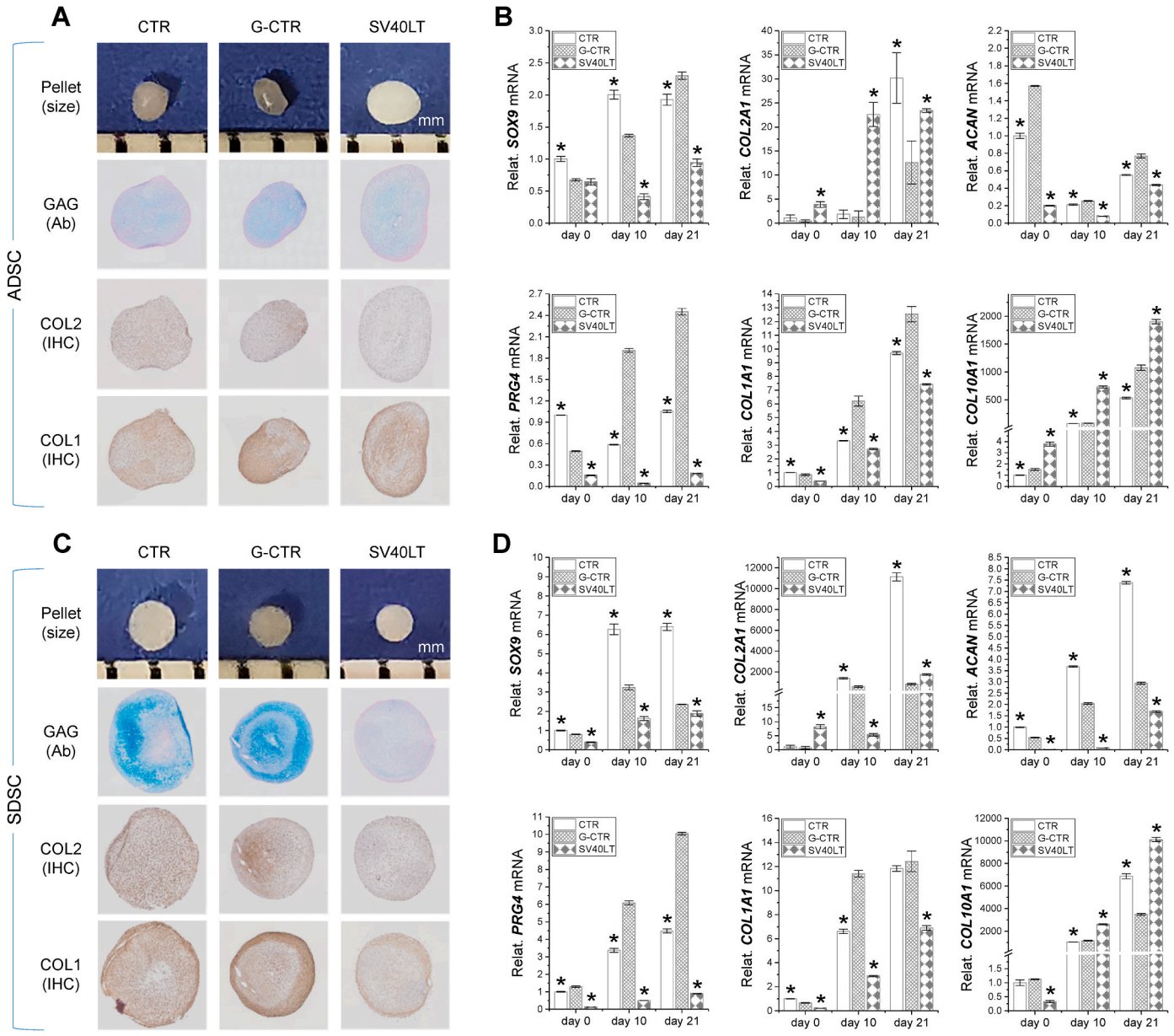

Fig. 2. Effect of SV40LT transduction on chondrogenic differentiation of human ADSCs and SDSCs. P8 ADSCs (A/B) and P9 SDSCs (C/D) were evaluated for their chondrogenic differentiation potential following transduction with either SV40LT (SV40LT) or GFP (G-CTR). Non-transduced cells were used as a control (CTR). (A/C) After 21 days of chondrogenic induction, pellets were stained with Alcian blue (Ab) for sulfated GAG and immunohistochemically (IHC) stained for collagens I and II. Scale bar: 500 μm. (B/D) The expression of chondrogenesis-related markers SOX9, COL1A1, COL2A1, COL10A1, ACAN, and PRG4 was quantified using TaqMan® qPCR. Data are presented in the form of bar charts. The symbol * denotes a statistically significant difference compared to the corresponding GFP-transduced control group (G-CTR, $P < 0.05$). (For interpretation of the references to colour in this figure legend, the reader is referred to the Web version of this article.)

during expansion and a gradual decrease during chondrogenic induction, dECM expansion in SDSCs dramatically upregulated TWIST1 expression, with the sECM group displaying the highest levels. This pattern was reversed during chondrogenic induction, with the sECM group showing the lowest expression.

3.4. Influence of GMdECMs on stem cell lineage differentiation

The differential responses of ADSCs and SDSCs to their respective dECM and GMdECM pretreatments were examined. Three dECM substrates, including cECM, gECM, and sECM, were used to expand the cells. The cells were then subjected to a 21-day incubation in chondrogenic medium. ADSC-derived pellets were observed to be of similar size but exhibited weaker staining for sulfated GAGs and collagen II compared to the respective SDSC groups, with the exception of collagen I immunostaining (Fig. 5A). Conversely, gECM-treated SDSC pellets were the smallest, while sECM-treated SDSC pellets were the largest, in line with the most intense staining of sulfated GAGs and collagen II and the least staining of collagen I (Fig. 5C).

RT–qPCR data revealed that ADSC pellets were less responsive to chondrogenic induction than SDSC pellets (Fig. 5B vs 5D). In ADSC pellets, the dECM groups demonstrated less response to chondrogenic induction compared to the TCP group, with the exception of COL10A1 expression (Fig. 5B). Interestingly, chondrogenicly induced pellets from both stem cell types showed reduced PRG4 expression in the dECM groups compared to the TCP group, with the sECM group demonstrating the lowest expression (Fig. 5B/D). In SDSC pellets, the dECM groups showed a greater response to chondrogenic induction than the TCP

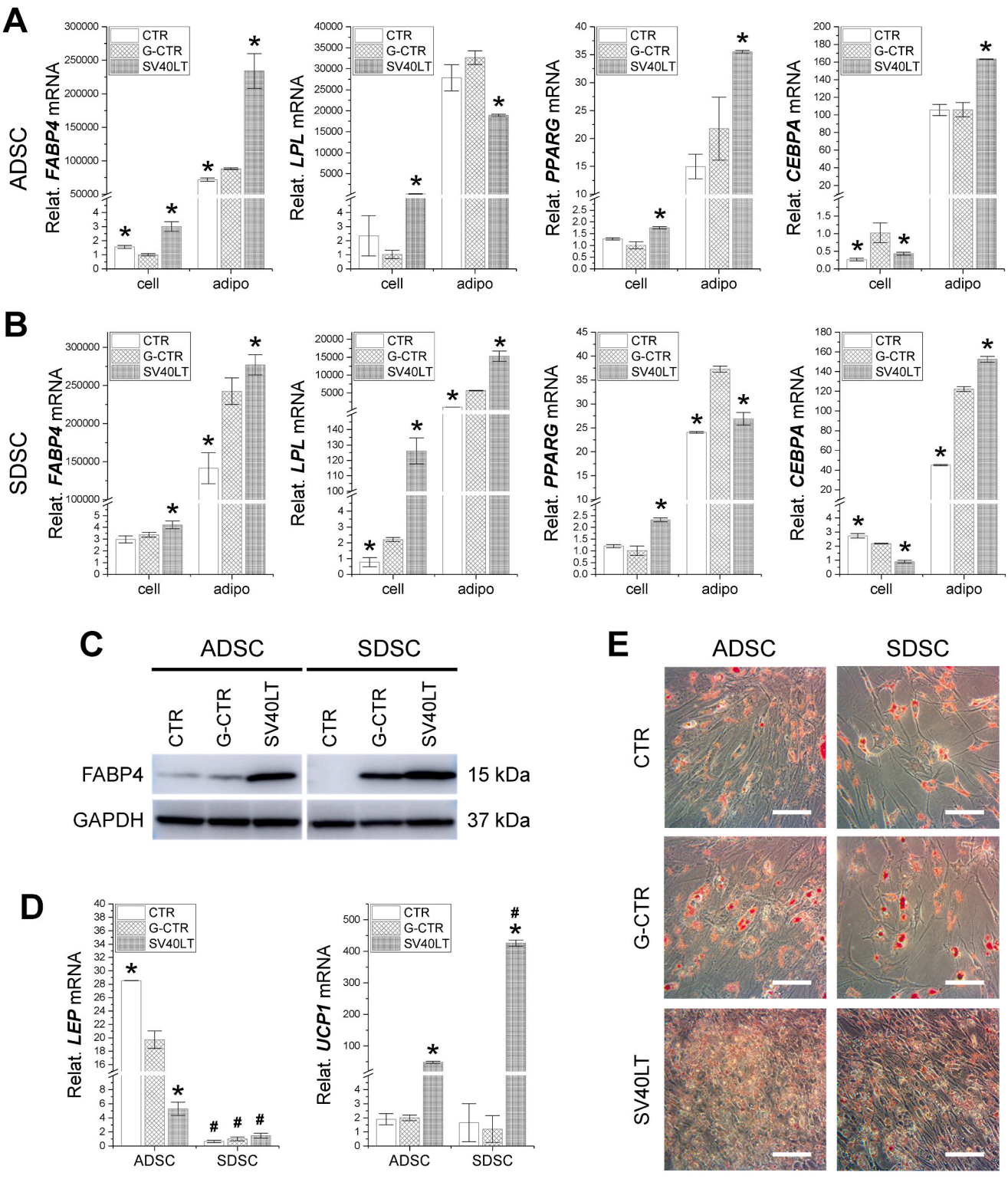

Fig. 3. Effect of SV40LT transduction on adipogenic differentiation of human ADSCs and SDSCs. Both P8 ADSCs and P9 SDSCs were evaluated for adipogenic differentiation capacity post-transduction with either SV40LT (SV40LT) or GFP (G-CTR), while non-transduced cells were used as controls (CTR). (A/B) TaqMan® qPCR was performed to quantify the expression of adipogenesis-related markers FABP4, LPL, PPARG, and CEBPA in ADSCs and SDSCs, which were induced for adipogenic differentiation for 21 days. Data are displayed as bar charts. The symbol * indicates a statistically significant difference compared to the corresponding GFP-transduced control group (G-CTR, $P < 0.05$). (C) Semiquantitative analysis of the expression of the adipogenic marker FABP4 was carried out using Western blotting, with GAPDH serving as an internal control. (D) The expression levels of the white adipose tissue marker gene LEP and brown adipose tissue marker gene UCP1 were quantified by TaqMan® qPCR. Data are shown as bar charts. The symbol * indicates a statistically significant difference compared to the corresponding GFP-transduced control group (G-CTR, $P < 0.05$), and the symbol # indicates a statistically significant difference from the corresponding ADSC group ($P < 0.05$). (E) Oil Red O staining was performed to visualize lipid droplets (scale bar = 100 μm). (For interpretation of the references to colour in this figure legend, the reader is referred to the Web version of this article.)

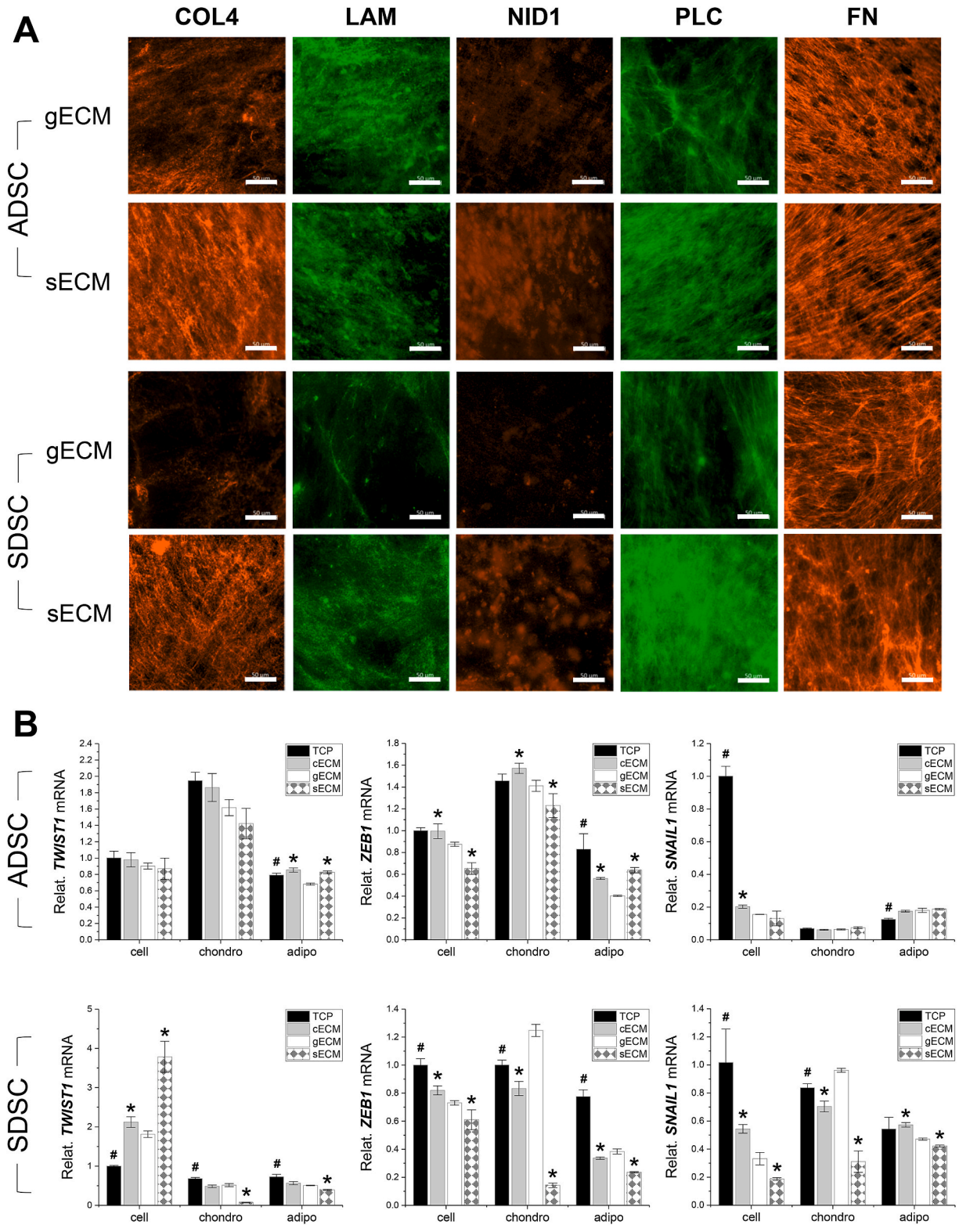

Fig. 4. Composition of decellularized extracellular matrix (dECM) and expression of EMT transcription factors during adipogenic and chondrogenic induction. (A) Assessment of the expression of basement membrane proteins, including Collagen IV (COL4), Laminin (LAM), Nidogen 1 (NID1), Perlecan (PLC), and Fibronectin (FN), in the dECMs laid down by ADSCs and SDSCs transduced with either SV40LT (sECM) or GFP (gECM). The scale bar represents 50 μm. (B) Evaluation of the dynamic changes in the expression levels of the EMT transcription factors TWIST1, ZEB1, and SNAIL1 during the chondrogenic and adipogenic induction of ADSCs and SDSCs. These cells were grown on dECMs deposited by their corresponding stem cells transduced with either SV40LT (sECM) or GFP (gECM). Non-transduced cells served as a control (cECM). Tissue Culture Plastic (TCP) was employed as a non-ECM control. The data are displayed as a bar chart, where the symbol * indicates a statistically significant difference compared to the GFP-transduced ECM control group (gECM, $P < 0.05$), and the symbol # signifies a statistically significant difference from the non-transduced ECM control group (cECM, $P < 0.05$).

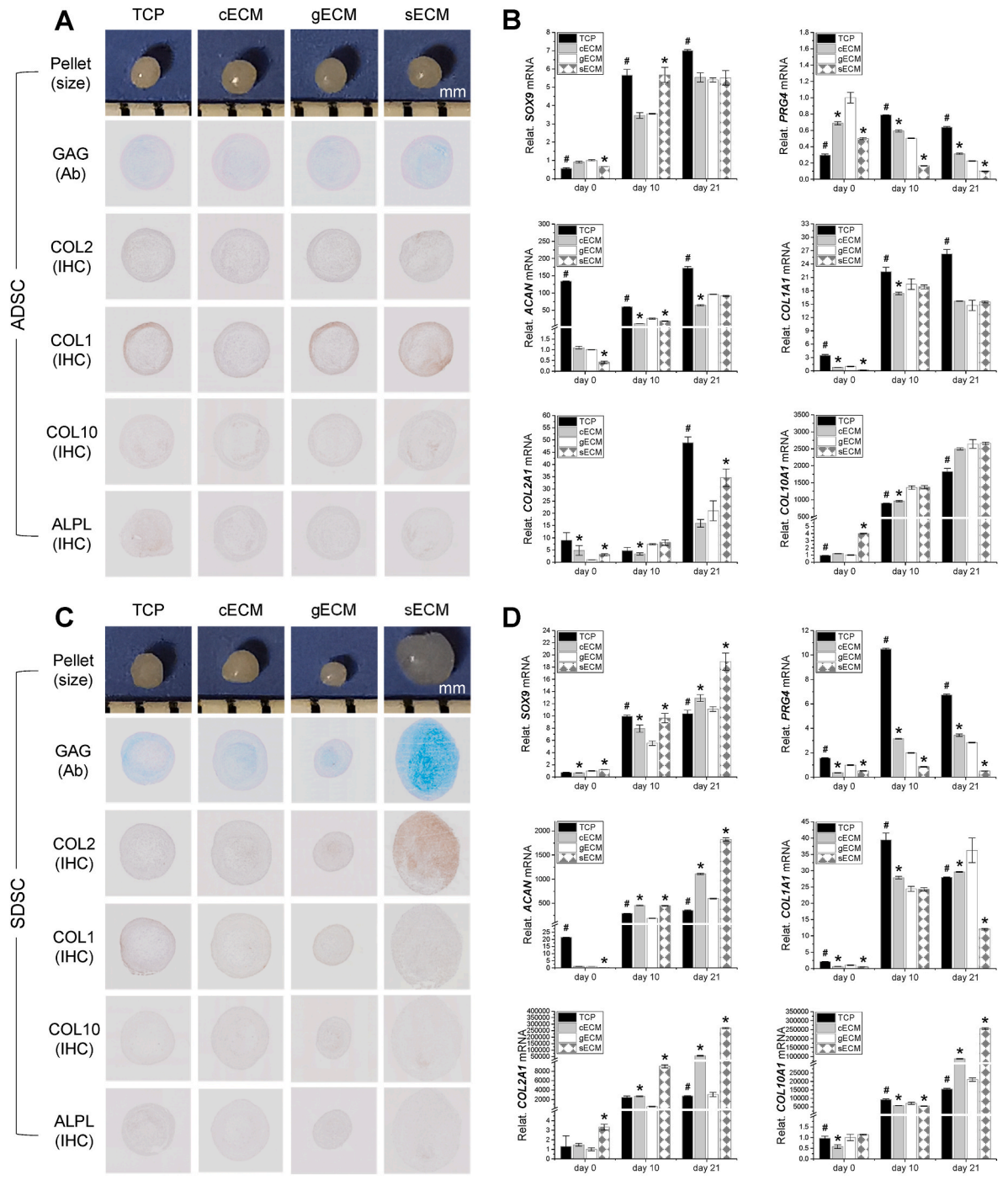

Fig. 5. Influence of the decellularized extracellular matrix (dECM) deposited by SV40LT-transduced ADSCs or SDSCs on the chondrogenic differentiation of corresponding stem cells. P5 ADSCs (A/B) and P6 SDSCs (C/D) were cultured for seven days on the dECM deposited by P8 ADSCs and P9 SDSCs following their transduction with either SV40LT (sECM) or GFP (gECM). Non-transduced cells served as a control (cECM), and tissue culture plastic (TCP) was employed as a non-ECM control. Following 21 days of chondrogenic induction, pellets were evaluated using Alcian blue staining (Ab) for the detection of sulfated glycosaminoglycans (GAGs) and immunohistochemical (IHC) staining for the presence of collagens I, II, and X (A/C). Scale bar: 500 μm. In parallel, TaqMan® qPCR was performed to evaluate the expression levels of chondrogenesis-related markers, including SOX9, COL1A1, COL2A1, COL10A1, ACAN, and PRG4 (B/D). Data are presented as a bar chart, where the symbol * denotes a statistically significant difference when compared with the GFP-transduced control group (G-CTR, $P < 0.05$). (For interpretation of the references to colour in this figure legend, the reader is referred to the Web version of this article.)

group, with the exception of COL1A1 expression (Fig. 5D), which is consistent with the immunohistochemistry data (Fig. 5C).

In a similar setup, the cells were exposed to a 21-day incubation in adipogenic medium. The dECM-expanded ADSCs produced more lipid droplets, while the dECM-expanded SDSCs produced fewer droplets (Fig. 6A), a trend that was confirmed by semiquantitative analysis of FABP4 using Western blotting (Fig. 6B). RT−qPCR data further confirmed that compared to the TCP group, dECM-expanded ADSCs showed an increase in adipogenic gene expression (FABP4, LPL, PPARG, CEBPA), with the sECM group showing the highest expression levels. In contrast, dECM-expanded SDSCs displayed reduced adipogenic gene expression, with the sECM group showing the lowest levels (FABP4, LPL,

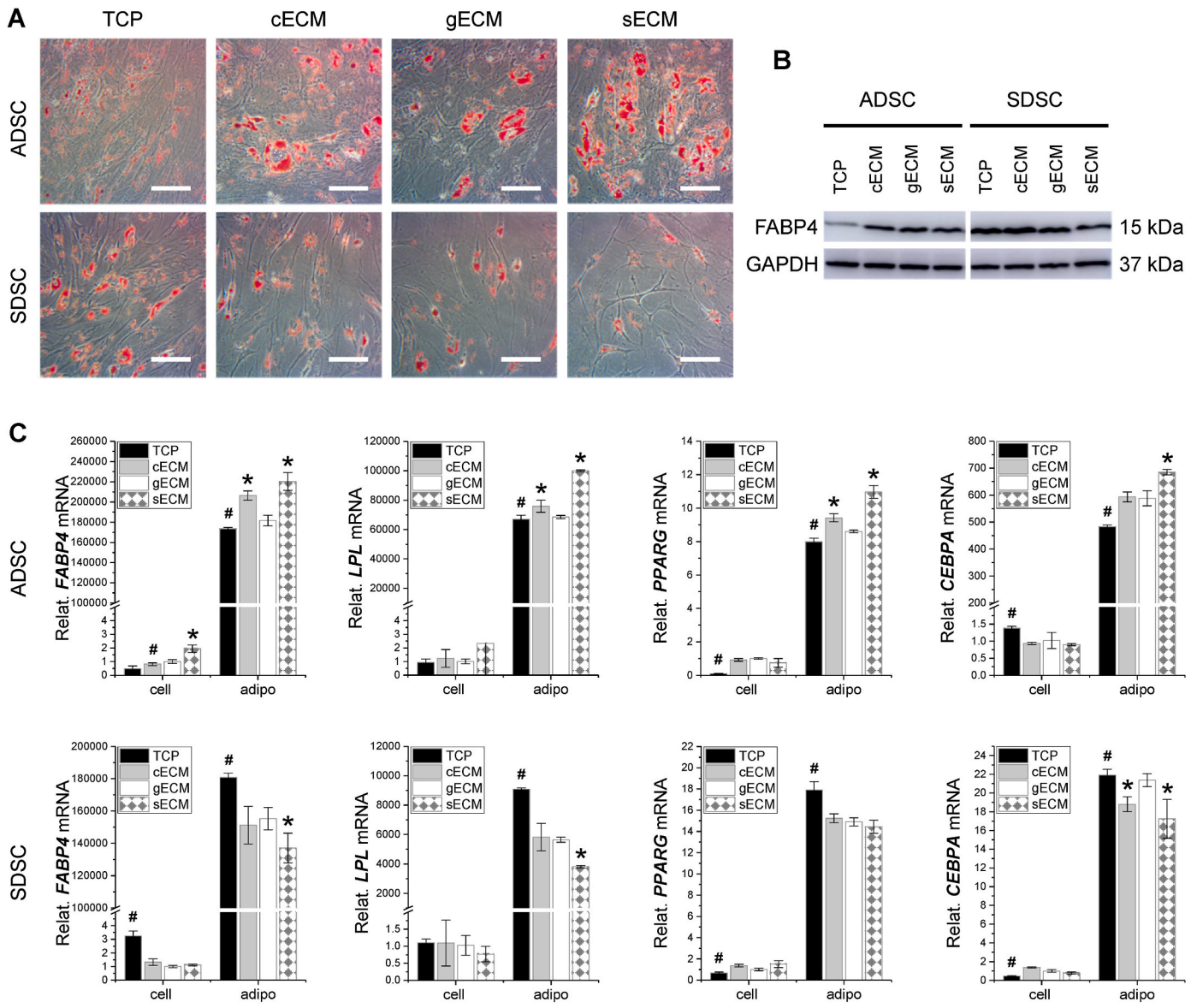

Fig. 6. Influence of the decellularized extracellular matrix (dECM) deposited by SV40LT-transduced ADSCs or SDSCs on the adipogenic differentiation of corresponding stem cells. P5 ADSCs and P6 SDSCs were cultured for seven days on the dECM deposited by P8 ADSCs and P9 SDSCs following their transduction with either SV40LT (sECM) or GFP (gECM). Non-transduced cells served as a control (cECM), and tissue culture plastic (TCP) was employed as a non-ECM control. After 21 days of adipogenic induction, the cells were evaluated using Oil Red O staining to identify lipid droplets (scale bar = 100 μm) (A) and Western blotting for the semi-quantification of the adipogenic marker FABP4, with GAPDH serving as the internal control (B). TaqMan® qPCR was conducted to evaluate the mRNA expression levels of adipogenesis-related markers FABP4, LPL, PPARG, and CEBPA in the expanded cells and the abiogenically induced cells (C). Data are presented as a bar chart. The symbol * denotes a statistically significant difference from the GFP-transduced control group (G-CTR, $P < 0.05$). (For interpretation of the references to colour in this figure legend, the reader is referred to the Web version of this article.)

CEBPA) (Fig. 6C).

3.5. Different responses of GMdECM-expanded ADSCs and SDSCs to chondrogenic induction

To further investigate whether sECM deposited by either ADSCs (AE40) or SDSCs (SE40) influenced the differentiation preference of expanded ADSCs and SDSCs, both cell types were expanded on TCP, SE40, and AE40 for seven days, followed by a 21-day chondrogenic induction in a pellet culture system. After *ex vivo* expansion on GMdECMs, both cell types exhibited a more fibroblast-like morphology with a polar distribution compared to their enlarged morphology when grown on TCP (Fig. 7A).

On the 21st day, ADSC pellets were slightly larger in the SE40 and AE40 groups than in the TCP group. However, positive staining was barely detectable in the ADSC pellets, including Ab staining for sulfated GAGs and IHC staining for collagen II (Fig. 7B). In contrast, the size of day 21 SDSC pellets in the TCP group was larger than that of the corresponding ADSC pellets. Pretreatment with both SE40 and AE40 significantly increased the size of SDSC pellets along with increased Ab staining for sulfated GAGs and IHC staining for collagen II, especially in the AE40 group (Fig. 7B).

The histological data aligned with the results from the RT–qPCR assay. SDSC pellets showed higher expression of COL2A1 in response to chondrogenic induction than the corresponding ADSC pellets, especially in both GMdECM groups (Fig. 7C).

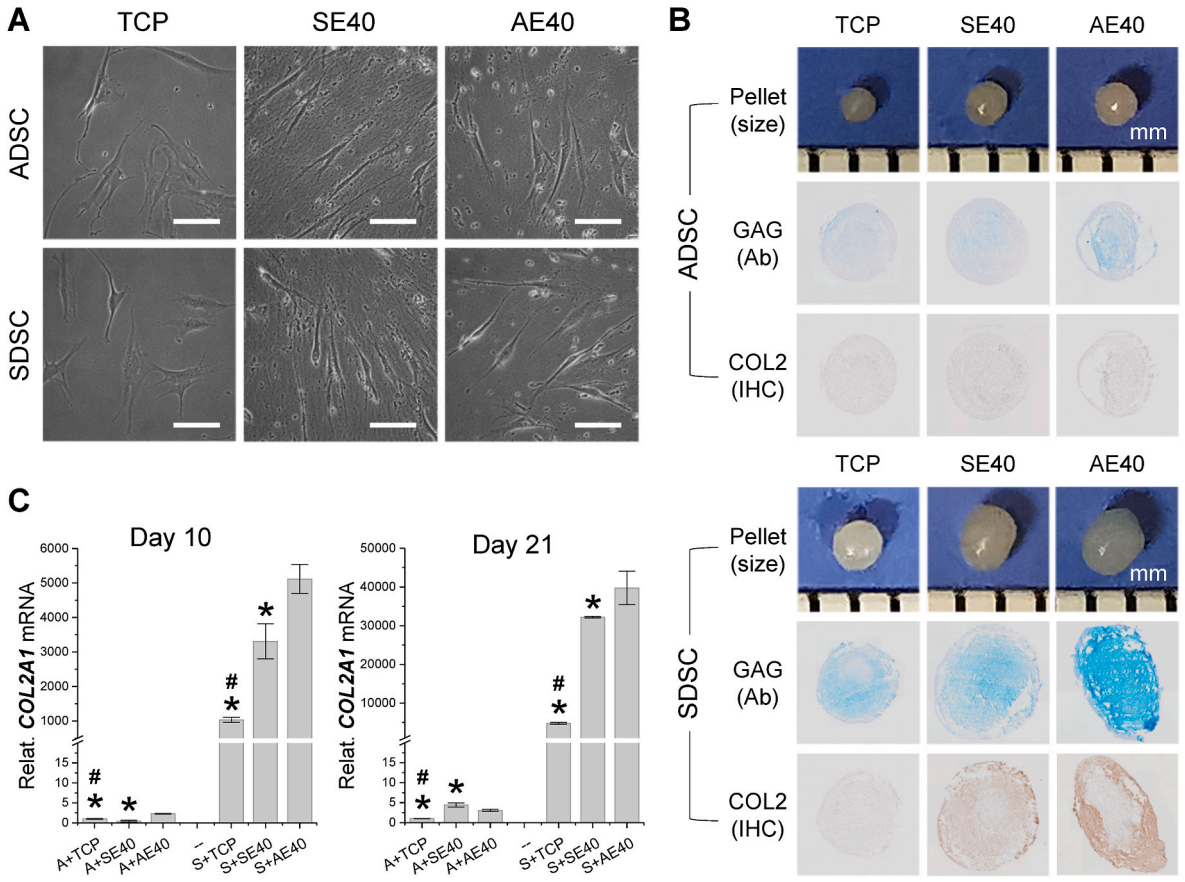

Fig. 7. Influence of the decellularized extracellular matrix (dECM) deposited by SV40LT-transduced ADSCs or SDSCs on the chondrogenic differentiation of corresponding stem cells. P5 ADSCs or P6 SDSCs were cultivated for seven days on the dECM laid down by P8 ADSCs or P9 SDSCs post-transduction with SV40LT (SE40) (scale bar = 100 μm) (A). Tissue culture plastic (TCP) functioned as a non-ECM control. Following 21 days of chondrogenic induction, pellets were assessed using Alcian blue staining (Ab) to detect sulfated glycosaminoglycans (GAGs) and immunohistochemistry (IHC) staining for collagen II (B). TaqMan® qPCR was utilized to gauge the expression of the chondrogenesis-related marker COL2A1 (C). Data are represented as a bar chart. The symbol * denotes a statistically significant difference from the ADSCs transduced with SV40LT group (AE40, $P < 0.05$), while the symbol # signifies a statistically significant difference from the SDSCs transduced with SV40LT group (SE40, $P < 0.05$). (For interpretation of the references to colour in this figure legend, the reader is referred to the Web version of this article.)

4. Discussion

Our findings are in line with a previous report using human IPFSCs [6], wherein both SV40LT-transduced human ADSCs and SDSCs showed decreased expression of CD73, CD90, and CD105 surface markers but increased expression of CD146 and enhanced EdU incorporation. Additionally, SV40LT-transduced ADSCs and SDSCs exhibited upregulated TP53 and CDKN2A (which encode p16 and p14ARF) but downregulated CDKN1A (encodes p21). Prior studies have shown that p14ARF activation results in the accumulation and stabilization of p53 [16], modulating p21 and triggering cell cycle arrest [17,18]. The observed changes in senescence gene expression along with CD146 upregulation [19] and increased EdU incorporation likely contributed to an increase in cell proliferation.

Interestingly, unlike our previous report where SV40LT-transduced human IPFSCs displayed upregulation of all evaluated stemness genes [6], SV40LT-transduced human SDSCs showed upregulation of SOX2, NANOG, NES, and MYC, downregulation of NOV and KLF4, and no significant change in POU5F1 and BMI1. Moreover, SV40LT-transduced human ADSCs exhibited upregulation of NES, POU5F1, and MYC, downregulation of SOX2, NANOG, and KLF4, and no significant change in BMI1 and NOV. The underlying mechanism for this discrepancy in the expression of stemness genes across different MSCs in response to SV40LT transduction remains unknown; it may influence their differentiation preference and warrants further investigation.

Our results showed that SDSCs transduced with SV40LT, despite being more sensitive to chondrogenic induction, showed decreased chondrogenic differentiation but increased adipogenic differentiation, which resembles the lineage preference of human IPFSCs after SV40LT transduction [6]. Interestingly, ADSCs and SDSCs exhibited opposing responses to chondrogenic and adipogenic induction when expanded on their own decellularized extracellular matrices (dECMs). Compared to cells grown on TCP, dECM-expanded cells exhibited a significantly lower level of ACAN expression. Notably, dECM-expanded SDSCs displayed an increased level of ACAN expression after chondrogenic induction, aligning with the dynamic expression of ACAN in human IPFSCs transduced with SV40LT [6].

These findings suggest that, similar to IPFSCs [6], SDSCs respond to the matrix environment in a manner expected of tissue-specific stem cells for chondrogenesis [9]. However, ADSCs responded differently to matrix pretreatment, showing lower expression of ACAN following chondrogenic induction. This discrepancy was also observed when considering their response to growth on GMdECMs. Following chondrogenic induction, GMdECM-expanded SDSCs, similar to IPFSCs [6], showed higher levels of chondrogenic markers SOX9, ACAN, and COL2A1 expression compared to those grown on dECMs. Conversely, GMdECM-expanded ADSCs did not respond well to chondrogenic induction, despite a slight increase in COL2A1.

Our adipogenic induction studies suggest that ADSCs tend to differentiate more toward white adipose tissue than SDSCs. Liu and colleagues, in a study using conditionally immortalized mouse and human brown preadipocytes (iBPAs), found that silencing SV40LT expression

prior to adipogenic induction was only necessary for inducing adipogenesis in human iBPAs, while their murine counterparts exhibited adipogenesis upon induction despite SV40LT expression [20]. In our model, we observed that SV40LT transduction promoted the differentiation of ADSCs and SDSCs toward brown adipose tissue, especially in SDSCs, which could partly be a result of TP53 upregulation in SDSCs/ADSCs transduced with SV40LT [21]. However, the reasons why SV40LT transduction did not hinder adipogenic differentiation in either ADSCs or SDSCs remain unclear.

Intriguingly, after expansion on dECM or GMdECM, ADSCs responded well to adipogenic induction, showing higher levels of adipogenic gene expression in the dECM group vs the TCP group and in the GMdECM group vs the dECM group. In contrast, SDSCs, after dECM and GMdECM expansion, did not respond well to adipogenic induction, demonstrating decreased levels of adipogenic gene expression in the dECM group (or GMdECM) vs the TCP group. The varied responses of ADSCs and SDSCs to the matrix microenvironment could possibly be due to tissue specificity, i.e., ADSCs are tissue-specific stem cells for adipogenesis, while SDSCs/IPFSCs are tissue-specific stem cells for chondrogenesis [7–10].

Additionally, the chondrogenic capability of ADSCs did not improve even after expansion on dECM deposited by SV40LT-transduced SDSCs, suggesting that while GMdECM can enhance lineage differentiation of tissue-specific stem cells, it does not significantly alter the differentiation preference of expanded stem cells. Similar to our previous findings showing the overexpression of basement membrane proteins in the dECM deposited by human IPFSCs transduced with SV40LT [6], more basement membrane proteins were detected in GMdECMs than in the corresponding dECMs in this study. This finding could be associated with the dynamic expression of EMT transcription factors, particularly TWIST1, in ADSCs and SDSCs following dECM/GMdECM expansion and chondrogenic induction.

The transcription factor TWIST1, a crucial regulator of mesenchymal cell fate, plays a significant and dynamic role in chondrogenesis. Its expression pattern, upregulated during the expansion phase and subsequently downregulated during differentiation, has been shown to boost chondrogenic differentiation of adult human bone marrow-derived mesenchymal stem cells (BMSCs) [22]. This dynamic fluctuation of TWIST1 during proliferation and chondrogenic induction correlates well with MSC proliferation, their uncommitted state [23,24], and chondrogenic potential [22], suggesting a role in maintaining stemness during proliferation and facilitating differentiation upon induction.

Our findings indicate that ADSCs demonstrate a steady TWIST1 expression pattern after expansion on both TCP and dECM substrates. In contrast, chondrogenic induction led to an increase in TWIST1 expression. Conversely, the dECM expansion phase significantly bolstered TWIST1 expression in SDSCs, especially in the GMdECM group, but a marked decrease was observed during chondrogenic induction, particularly in the dECM and GMdECM groups.

TWIST1 is known to be pivotal in limb bud mesenchyme by inhibiting SOX9 [25] and RUNX2 [26]. Consequently, the minimal TWIST1 expression in GMdECM-expanded SDSCs post-chondrogenic induction might be driving the highest expression of SOX9 (essential for chondrogenesis) and COL10A1 (a marker for chondrocyte hypertrophy) [27]. This correlation aligns with the understanding that TWIST1 is integral to immature chondrocytes, mainly due to its inhibitory effect on RUNX2, which prevents further differentiation toward hypertrophy [27].

Notably, we observed a downregulation of both ZEB1 and SNAIL1 in chondrogenicly induced SDSCs expanded on the dECM deposited by SV40LT-transduced cells, which could be linked to their reported inhibitory effects on chondrogenic differentiation [28,29]. Collectively, these findings lend support to the idea that SDSCs are more aligned with tissue-specific stem cells for chondrogenesis than ADSCs.

In essence, our study adds to the growing body of evidence highlighting the pivotal roles of specific transcription factors such as TWIST1, ZEB1, and SNAIL1 in directing the lineage commitment of stem cells and underscores the nuanced roles of the matrix microenvironment in guiding stem cell behavior.

5. Conclusion

In conclusion, our work suggests that although the matrix microenvironment influences tissue-specific stem cell behavior, it does not determine their lineage differentiation preference. Compared to dECM, GMdECM provides a more potent matrix environment, enhancing the capacity of SDSCs and ADSCs for cartilage and adipose tissue regeneration, respectively. Our findings could be significant for understanding stem cell behavior and enhancing tissue-specific stem cell potential for regenerative medicine applications.

Funding

This work was supported by a grant from the National Institutes of Health, United States (Grant No. AR078846).

Declaration of competing interest

The authors declare that they have no known competing financial interests or personal relationships that could have appeared to influence the work reported in this paper.

Data availability

Data will be made available on request.

Acknowledgments

We thank Suzanne Danley for editing the manuscript.

References

[1] W.S. Toh, C.B. Foldager, M. Pei, J.H. Hui, Advances in mesenchymal stem cell-based strategies for cartilage repair and regeneration, Stem Cell Rev. Rep. 10 (2014) 686–696.
[2] J. Li, M. Pei, Cell senescence: a challenge in cartilage engineering and regeneration, Tissue Eng., Part B 18 (2012) 270–287.
[3] C. Liu, M. Pei, Q. Li, Y. Zhang, Decellularized extracellular matrix mediates tissue construction and regeneration, Front. Med. 16 (2022) 56–82.
[4] M. Pei, J. Li, M. Shoukry, Y. Zhang, A review of decellularized stem cell matrix: a novel cell expansion system for cartilage tissue engineering, Eur. Cell. Mater. 22 (2011) 333–343, discussion 343.
[5] M. Pei, Environmental preconditioning rejuvenates adult stem cells' proliferation and chondrogenic potential, Biomaterials 117 (2017) 10–23.
[6] Y. Wang, G.Q. Hu, R.C. Hill, M. Dzieciatkowska, K.C. Hansen, X.B. Zhang, Z.Q. Yan, M. Pei, Matrix reverses immortalization-mediated stem cell fate determination, Biomaterials 265 (2021), 120387.
[7] Y. Wang, S. Chen, Z. Yan, M. Pei, A prospect of cell immortalization combined with matrix microenvironmental optimization strategy for tissue engineering and regeneration, Cell Biosci. 9 (2019) 7.
[8] T. Wang, R.C. Hill, M. Dzieciatkowska, L. Zhu, A.M. Infante, G. Hu, K.C. Hansen, M. Pei, Site-dependent lineage preference of adipose stem cells, Front. Cell Dev. Biol. 8 (2020) 237.
[9] B.A. Jones, M. Pei, Synovium-derived stem cells: a tissue-specific stem cell for cartilage engineering and regeneration, Tissue Eng., Part B 18 (2012) 301–311.
[10] T. Pizzute, K. Lynch, M. Pei, Impact of tissue-specific stem cells on lineage-specific differentiation: a focus on the musculoskeletal system, Stem Cell Rev. Rep. 11 (2015) 119–132.
[11] Y. Wang, Y.A. Pei, Y. Sun, S. Zhou, X.B. Zhang, M. Pei, Stem cells immortalized by hTERT perform differently from those immortalized by SV40LT in proliferation, differentiation, and reconstruction of matrix microenvironment, Acta Biomater. 136 (2021) 184–198.
[12] J. Li, K. Narayanan, Y. Zhang, R.C. Hill, F. He, K.C. Hansen, M. Pei, Role of lineage-specific matrix in stem cell chondrogenesis, Biomaterials 231 (2020), 119681.
[13] M. Pei, Y.A. Pei, S. Zhou, E. Mikaeiliagah, C. Erickson, B. Giertych, K. Akhter, L. Wang, A. Stewart, J. Parenti, B. Wang, S. Wen, S. Sim, E. Quenneville, K. C. Hansen, S. Frisch, G. Hu, Matrix from urine stem cells boosts tissue-specific stem cell mediated functional cartilage reconstruction, Bioact. Mater. 23 (2022) 353–367.
[14] J. Li, M. Pei, A protocol to prepare decellularized stem cell matrix for rejuvenation of cell expansion and cartilage regeneration, Methods Mol. Biol. 1577 (2018) 147–154.

[15] T. Pizzute, Y. Zhang, F. He, M. Pei, Ascorbate-dependent impact on cell-derived matrix in modulation of stiffness and rejuvenation of infrapatellar fat derived stem cells toward chondrogenesis, Biomed. Mater. 11 (2016), 045009.
[16] Y. Zhang, Y. Xiong, W.G. Yarbrough, ARF promotes MDM2 degradation and stabilizes p53: ARF-INK4a locus deletion impairs both the Rb and p53 tumor suppression pathways, Cell 92 (1998) 725–734.
[17] A.B. Niculescu 3rd, X. Chen, M. Smeets, L. Hengst, C. Prives, S.I. Reed, Effects of p21(Cip1/Waf1) at both the G1/S and the G2/M cell cycle transitions: pRb is a critical determinant in blocking DNA replication and in preventing endoreduplication, Mol. Cell Biol. 18 (1998) 629–643.
[18] F. Bunz, A. Dutriaux, C. Lengauer, T. Waldman, S. Zhou, J.P. Brown, J.M. Sedivy, K.W. Kinzler, B. Vogelstein, Requirement for p53 and p21 to sustain G2 arrest after DNA damage, Science 282 (1998) 1497–1501.
[19] M. Matsui, T. Kobayashi, T.W. Tsutsui, CD146 positive human dental pulp stem cells promote regeneration of dentin/pulp-like structures, Hum. Cell 31 (2018) 127–138.
[20] J. Liu, E.N. Kuipers, H.C.M. Sips, J.C. Dorleijn, A.D. van Dam, C. Christodoulides, F. Karpe, G. Zhou, M.R. Boon, P.C.N. Rensen, A.A.F. de Vries, S. Kooijman, Conditionally immortalized brown preadipocytes can switch between proliferative and differentiated states, Biochim. Biophys. Acta Mol. Cell Biol. Lipids 1864 (2019), 158511.
[21] A. Molchadsky, O. Ezra, P.G. Amendola, D. Krantz, I. Kogan-Sakin, Y. Buganim, N. Rivlin, N. Goldfinger, V. Folgiero, R. Falcioni, R. Sarig, V. Rotter, p53 is required for brown adipogenic differentiation and has a protective role against diet-induced obesity, Cell Death Differ. 20 (2013) 774–783.
[22] M.A. Cleary, R. Narcisi, A. Albiero, F. Jenner, L.M.G. de Kroon, W.J.L.M. Koevoet, P.A.J. Brama, G.J.V.M. van Osch, Dynamic regulation of TWIST1 expression during chondrogenic differentiation of human bone marrow-derived mesenchymal stem cells, Stem Cell. Dev. 26 (2017) 751–761.
[23] S. Isenmann, A. Arthur, A.C. Zannettino, J.L. Turner, S. Shi, C.A. Glackin, S. Gronthos, TWIST family of basic helix-loop-helix transcription factors mediate human mesenchymal stem cell growth and commitment, Stem Cell. 27 (2009) 2457–2468.
[24] R. Narcisi, M.A. Cleary, P.A. Brama, M.J. Hoogduijn, N. Tüysüz, D. ten Berge, G. J. van Osch, Long-term expansion, enhanced chondrogenic potential, and suppression of endochondral ossification of adult human MSCs via WNT signaling modulation, Stem Cell Rep. 4 (2015) 459–472.
[25] S. Gu, T.G. Boyer, M.C. Naski, Basic helix-loop-helix transcription factor Twist1 inhibits transactivator function of master chondrogenic regulator Sox9, J. Biol. Chem. 287 (2012) 21082–21092.
[26] P. Bialek, B. Kern, X. Yang, M. Schrock, D. Sosic, N. Hong, H. Wu, K. Yu, D. M. Ornitz, E.N. Olson, M.J. Justice, G. Karsenty, A twist code determines the onset of osteoblast differentiation, Dev. Cell 6 (2004) 423–435.
[27] Y.F. Dong, D.Y. Soung, Y. Chang, M. Enomoto-Iwamoto, M. Paris, R.J. O'Keefe, E. M. Schwarz, H. Drissi, Transforming growth factor-beta and Wnt signals regulate chondrocyte differentiation through Twist1 in a stage-specific manner, Mol. Endocrinol. 21 (2007) 2805–2820.
[28] K. Seki, T. Fujimori, P. Savagner, A. Hata, T. Aikawa, N. Ogata, Y. Nabeshima, L. Kaechoong, Mouse Snail family transcription repressors regulate chondrocyte, extracellular matrix, type II collagen, and aggrecan, J. Biol. Chem. 278 (2003) 41862–41870.
[29] H. Swahn, K. Li, T. Duffy, M. Olmer, D.D. D'Lima, T.S. Mondala, P. Natarajan, S. R. Head, M.K. Lotz, Senescent cell population with ZEB1 transcription factor as its main regulator promotes osteoarthritis in cartilage and meniscus, Ann. Rheum. Dis. 82 (2023) 403–415.